Environmental Science & Technology

Article

pubs.acs.org/est

Visible-Light-Driven Photocatalytic Inactivation of *E. coli* K-12 by Bismuth Vanadate Nanotubes: Bactericidal Performance and Mechanism

Wanjun Wang,[†] Ying Yu,*[,‡] Taicheng An,[§] Guiying Li,[§] Ho Yin Yip,[†] Jimmy C. Yu,[∥] and Po Keung Wong*[,†]

[†]School of Life Sciences and [∥]Department of Chemistry, The Chinese University of Hong Kong, Shatin, N.T., Hong Kong SAR, China

[‡]Institute of Nanoscience and Nanotechnology, Central China Normal University, Wuhan 430079, China

[§]State Key Laboratory of Organic Geochemistry, Guangzhou Institute of Geochemistry, Chinese Academy of Sciences, Guangzhou 510640, China

Supporting Information

ABSTRACT: Bismuth vanadate nanotube (BV-NT), synthesized by a template-free solvothermal method, was used as an effective visible-light-driven (VLD) photocatalyst for inactivation of *Escherichia coli* K-12. The mechanism of photocatalytic bacterial inactivation was investigated by employing multiple scavengers combined with a simple partition system. The VLD photocatalytic bacterial inactivation by BV-NT did not allow any bacterial regrowth. The photogenerated h^+ and reactive oxidative species derived from h^+, such as $\bullet OH_{ads}$, H_2O_2 and $\bullet HO_2/\bullet O_2^-$, were the major reactive species for bacterial inactivation. The inactivation by h^+ and $\bullet OH_{ads}$ required close contact between the BV-NT and bacterial cells, and only a limited amount of H_2O_2 could diffuse into the solution to inactivate bacterial cells. The direct oxidation effect of h^+ to bacterial cells was confirmed by adopting F^- surface modification and anaerobic experiments. The bacterial cells could trap e^- in order to minimize e^--h^+ recombination, especially under anaerobic condition. Transmission electron microscopic study indicated the destruction process of bacterial cell began from the cell wall to other cellular components. The $\bullet OH_{ads}$ was postulated to be more important than $\bullet OH_{bulk}$ and was not supposed to be released very easily in the BV-NT bacterial inactivation system.

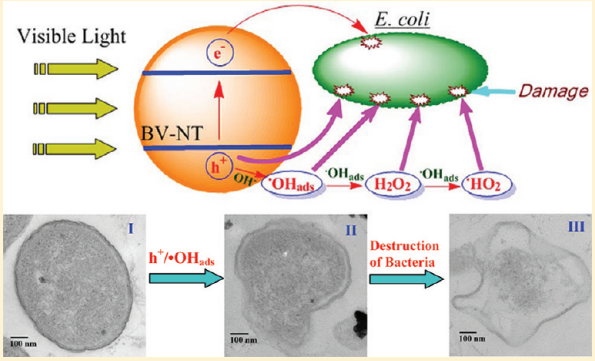

1. INTRODUCTION

Since the discovery of photocatalytic inactivation of microbial cells with TiO_2 by Matsunaga et al. in 1985,[1] semiconductor-based materials have been extensively investigated as photocatalysts for bacterial inactivation.[2,3] However, the most widely used TiO_2 photocatalyst is only active under UV irradiation which accounts for only 4% of the sunlight spectrum, while 45% of the sunlight spectrum is visible light (VL). Since doped modification and composite TiO_2 extending the light absorption to VL region, thus leading to the complicated fabrication procedure to adjust the components, many researchers have turned their focus on novel non-TiO_2 based single-phase VLD photocatalysts. Bismuth vanadate ($BiVO_4$) is one of the most promising VL-responsive photocatalysts. Unfortunately, most of the studies about $BiVO_4$ only focus on photocatalytic evolution of O_2 or degradation of organic pollutants,[4,5] and the work on water disinfection is very limited. However, its excellent photocatalytic degradation activity suggested that $BiVO_4$ might have high VLD photocatalytic bacterial inactivation ability. For UV-irradiated TiO_2 system, major reactive species responsible for destruction of microorganisms are often proposed to be hydroxyl radical ($\bullet OH$), which is either adsorbed on TiO_2 surface (i.e., $\bullet OH_{ads}$) or free in bulk solution (i.e., $\bullet OH_{bulk}$). However, the fundamental mechanism underlying the VLD photocatalytic inactivation process, especially in non-TiO_2 based system, has not been well-established. For example, controversy still exists over (1) whether the direct hole (h^+) oxidation plays a major role, and (2) whether the $\bullet OH_{ads}$ can release into the bulk solution to become $\bullet OH_{bulk}$. It is well-known that for an effective photocatalytic degradation process, the direct contact between pollutants and photocatalysts is important.[6] However, for the destruction of microorganisms, such as MS-2 phage can be inactivated mainly by $\bullet OH_{bulk}$ in the bulk solution without direct contact with the photocatalysts.[7] In our previous study, it

Received: December 1, 2011
Revised: February 3, 2012
Accepted: March 19, 2012
Published: March 19, 2012

   dx.doi.org/10.1021/es2042977 | Environ. Sci. Technol. 2012, 46, 4599–4606

is also found that *Escherichia coli* K-12 can be effectively inactivated inside a semipermeable membrane system (i.e., a partition system) by H_2O_2 diffusion in the presence of B−Ni-codoped TiO_2 under VL irradiation.[8] These studies indicated that direct contact was not required for photocatalytic inactivation of *E. coli* K-12. But it is still premature to conclude that is the generalization for photocatalytic bacterial inactivation, since it may only be valid for TiO_2-based photocatalysts.

Recently, monoclinic structured $BiVO_4$ nanotube (BV-NT) has been synthesized by a facile one-pot template-free solvothermal method.[9] The as-prepared sample shows remarkable photocatalytic activity for water splitting and Rhodamine B (RhB) degradation under VL irradiation.[9,10] Herein, we further systematically investigated the photocatalytic inactivation of *E. coli* K-12 by using the as-prepared BV-NT as a VLD photocatalyst. Scavengers for different reactive charged (i.e., e^- and h^+) and oxidative (i.e., •OH and H_2O_2) species were employed to investigate the roles of these species in the VLD photocatalytic inactivation process. Moreover, a simple partition system with a semipermeable membrane[6,8] to separate photocatalyst from bacterial cells was employed to determine whether the direct contact between the photocatalyst and bacterial cell is required for the inactivation.

2. EXPERIMENTAL SECTION

2.1. Materials. The BV-NT photocatalysts used in this study were prepared by a solvothermal method, and the detail synthesis procedure can be found in our previous study.[9,10] The as-prepared BV-NT showed monoclinic structure with lattice constants of a = 0.5191 nm, b = 1.1712 nm, and c = 0.5103 nm. The obtained nanotubes had hexagonal cross sections with long lengths of 1.2 μm, side lengths of 200 nm, and wall thicknesses of 30 nm. Typical field-emission scanning electron microscopy (FESEM, JEOL, JSM-6700F) and transmission electron microscopy (TEM, FEI Tecnai G2 Spirit) images of the as-prepared sample were shown in Figure 1(A) and 1(B), respectively. The bandgap energy of BV-NT was estimated to be 2.53 eV by UV−vis diffuse reflectance spectroscopy (DRS).[9] Potassium dichromate [$K_2Cr_2O_7$ (Cr(VI)], sodium fluoride (NaF), sodium oxalate ($Na_2C_2O_4$), and isopropanol ($(CH_3)_2CHOH$) were purchased from Riedel-deHaën Chemical Co. (Germany). Ferric sulfate-ethylenediamine-tetraacetic acid [$FeSO_4$-EDTA (Fe(II)] was purchased from AJAX Chemicals (Australia). 4-Hydroxy-2,2,6,6-tetramethylpiperidinyloxy (TEMPOL) was obtained from Sigma Chemical Co. (USA). All of the chemicals were of analytical reagent grade, and isopropanol was of HPLC grade and dehydrated.

2.2. Photocatalytic Inactivation. The VLD photocatalytic inactivation of *E. coli* K-12 was conducted using a 300 W xenon lamp (Beijing Perfect Light Co. Ltd., Beijing) with a UV cutoff filter (λ < 400 nm) as light source. The VL intensity was measured by a light meter (LI-COR, USA), and the light intensity for the experiments was fixed at 193 mW/cm^2. All glass apparatuses used in the experiments were autoclaved at 121 °C for 20 min to ensure sterility. The bacterial cells were cultured in nutrient broth (Lancashire, UK) at 37 °C and agitated at 200 rpm for 16 h. The cultures were then washed twice with sterilized saline (0.9% NaCl) solution by centrifugation for 5 min, and then the cell pellet was resuspended in sterilized saline solution. The photocatalyst and the saline suspension of washed cell were then added into a flask with an aluminum cover. The final cell density was adjusted to about 2 × 10^5 cfu (colony forming unit)/mL. The reaction temperature was maintained at 25 °C, and the reaction mixture was stirred with a magnetic stirrer throughout the experiment. At different time intervals, aliquots of the sample were collected and serially diluted with sterilized saline solution. 0.1 mL of the diluted sample was then immediately spread on nutrient agar (Lancashire, UK) plates and incubated at 37 °C for 24 h to determine the number of viable cells (in cfu). Before irradiation, the suspensions were magnetically stirred in the dark for 60 min to ensure the establishment of an adsorption/desorption equilibrium between the photocatalyst and bacterial cells. For comparison, three control experiments were conducted along with treatment experiments. The dark control was carried out with BV-NT alone in the dark, light control in the absence of BV-NT under VL irradiation, and negative control without BV-NT or VL irradiation. All the treatment and control experiments were performed in triplicates.

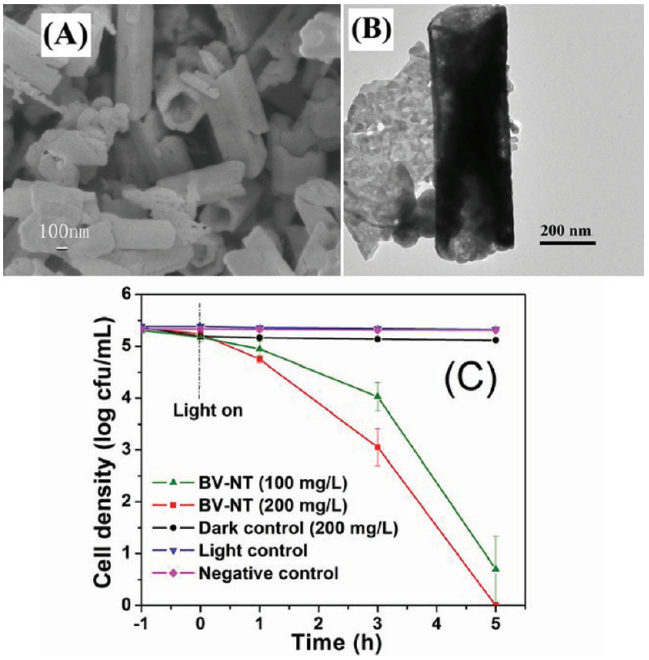

Figure 1. (A) Typical SEM image and (B) TEM image of the as-prepared BV-NT and (C) photocatalytic inactivation efficiency of *E. coli* K-12 (2 × 10^5 cfu/mL, 50 mL) under VL irradiation in the presence of BV-NT.

The setup of the partition system for this experiment is shown in Figure S1. The semipermeable membrane used in the study was regenerate cellulose (RC) membrane purchased from Spectrum Laboratories, Inc. (USA). Twenty mL of *E. coli* K-12 saline suspension (2 × 10^5 cfu/mL) was pipetted into the semipermeable container, and the outside of the membrane was 50 mL of the BV-NT saline suspension (100 mg/L), which was stirred continuously to keep the BV-NT evenly distributed in the solution outside of the membrane. At different time intervals, aliquots of the cells inside the membrane were sampled and immediately diluted to determine the number of viable cells.

2.3. Analysis of Reactive Species. The generation of •OH was investigated through the method of photoluminescence with terephthalic acid. The •OH was captured by terephthalic acid to produce a fluorescent product 2-hydroxyterephthalic acid[11] and then analyzed by a fluorescence spectrophotometer (Tecan, Männedorf, Switzerland, excitation wavelength: 315 nm; fluorescence peak: 425 nm). Hydrogen

peroxide (H_2O_2) was analyzed photometrically by the POD (horseradish peroxidase)-catalyzed oxidation product of DPD (N,N-diethyl-*p*-phenylenediamine) at 551 nm.[12] For the surface analysis of F^- modified BV-NT, XPS experiments were performed on a Physical Electronics PHI 5600 multi-technique system, using monochromatized Al Kα radiation (1486.6 eV) at 350 W. All the binding energies were calibrated to the C 1s peak at 284.8 eV of surface adventitious carbon.

2.4. Preparation Procedure for Bacterial TEM Study. The mixture of the BV-NT and *E. coli* K-12 before and after photocatalytic inactivation was collected and centrifuged. The bacterial cells were prefixed by 2.5% glutaraldehyde and trapped in 3% low melting point agarose. After being postfixed by 1% osmium tetraoxide (E.M. grade, Electron Microscopy Sciences, Fort Washington, PA, USA) in phosphate buffer (0.1 M, pH 7.2), the cell pellet was dehydrated by adding a graded series of ethanol and finally embedded in Spurr solution (Electron Microscopy Sciences, Fort Washington, PA, USA) for polymerization at 68 °C. By using an ultramicrotome (Leica, Reichert Ultracuts, Wien, Austria), ultrathin sections of 70 nm were made and stained with uranyl acetate and lead citrate on copper grids. Finally, the stained ultrathin sections were examined by a JEM-1200 EXII transmission electron microscope (JEOL Ltd., Tokyo, Japan).

2.5. Analysis of Bacterial Catalase Activity and Potassium Ions. Catalase (CAT) activity determination was conducted using the Catalase Assay Kit (Cayman Chemical Company, Ann Arbor, MI, USA), following the protocol recommended by the manufacturer.[13] One unit of CAT activity (nmol/min/mL) was defined as the amount of enzyme that would cause the formation of 1.0 nmol of formaldehyde per minute at 25 °C. To investigate K^+ leakage from the bacterial cells during the photocatalytic inactivation process, the BV-NT/bacterial cell suspension before and after inactivation treatment was collected and filtered through a Millipore filter (pore size of 0.45 μm). After filtration, the K^+ concentration in the resulting clear solution was measured by a polarized Zeeman atomic absorption spectrophotometer (AAS) (Hitachi Z-2300, Japan). All the above experiments were also conducted in triplicates.

3. RESULTS AND DISCUSSION

3.1. Photocatalytic Inactivation. The VLD photocatalytic inactivation efficiencies of *E. coli* K-12 by BV-NT with different concentration of photocatalyst are shown in Figure 1(C). In the dark, light, and negative control experiments, the bacterial population remained unchanged even after 5 h, indicating no toxic effect of BV-NT to *E. coli* K-12 cells and no photolysis of bacterial cells under VL irradiation alone. However, with VL irradiation plus photocatalyst, the 100 mg/L BV-NT exhibited high photocatalytic activity to inactivate bacterial cells and ~4 log of *E. coli* K-12 was inactivated after 5 h irradiation. When further increasing the photocatalyst concentration to 200 mg/L, the inactivation efficiency was proportionally increased and the complete inactivation of *E. coli* was achieved within 5 h irradiation, indicating that the photocatalytic efficiency is dependent on the photocatalyst concentration and BV-NT is a true VLD photocatalyst for bacterial inactivation with high efficiency.

Bacterial regrowth test was conducted to evaluate the effectiveness of bacterial inactivation by the photocatalytic process. Complete inactivation of *E. coli* K-12 (2×10^5 cfu/mL) was achieved within 5 h of VL irradiation with 200 mg/L BV-NT. After the corresponding photocatalytic inactivation treatments, the reaction mixture was sampled and underwent a 96 h recovery period to determine the bacterial regrowth. Results (data not shown) indicated that no detectable bacterial count (in cfu/mL) was observed after 96 h incubation period. It suggests that 5 h is an effective disinfection time (EDT)[14] for VLD photocatalytic inactivation of *E. coli* K-12 by BV-NT, which is defined as the time required for complete bacterial inactivation without regrowth in a subsequent dark period for 96 h. This result also suggests that photocatalytic inactivation by the BV-NT lead to irreversible damage to *E. coli* K-12. Thus, VLD photocatalytic disinfection is a safe and effective method to eliminate water-borne bacterium such as *E. coli*. Compared with the tedious fabrication procedures of doped and composite TiO_2, this one-pot synthesized single phase VLD photocatalyst is much applicable to be produced in large-scale for water disinfection treatment.

3.2.1. Mechanism of Photocatalytic Inactivation. *Role of Primary Reactive Species.* To find out which reactive species play more significant role(s) in the VLD bacterial inactivation by BV-NT, the scavenging study was performed, which employed different scavengers individually to remove the specific reactive species. The scavengers used in this study were sodium oxalate for h^+,[15,16] isopropanol for $\bullet OH_{bulk}$,[17,18] Cr(VI) for e^-,[17,19] and Fe(II) for H_2O_2.[16,20] Before conducting the experiment, the applied concentration of each scavenger was optimized to ensure their maximum scavenging effect but did not cause any inactivation to the bacterial cell.[8] No bacterial inactivation occurs in dark and light controls (Figure S2). Isopropanol is a well-known scavenger for $\bullet OH$ with a rate constant of 1.9×10^9 M^{-1} s^{-1}, which is almost equal to the diffusion limit.[21] Because of its poor affinity to photocatalyst surface, isopropanol is usually used as a diagnostic tool of $\bullet OH_{bulk}$ mediated mechanism. With the addition of isopropanol, the inactivation efficiency remains almost the same as that of no scavenger (Figure 2), indicating a small amount of $\bullet OH_{bulk}$ is involved in the VLD photocatalytic inactivation process. Meanwhile, no inhibition effect is observed when utilizing Cr(VI) as the scavenger to quench the reactive species in the reduction pathway, and the inactivation efficiency becomes even better than that of no scavenger. This result

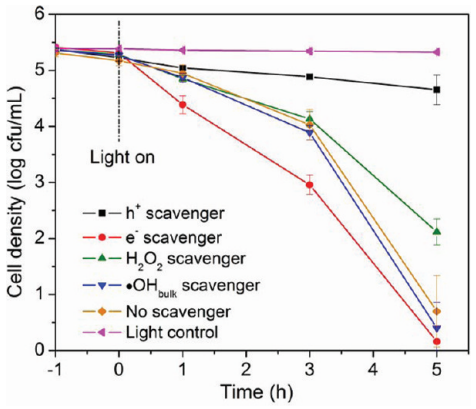

Figure 2. Photocatalytic inactivation efficiency of *E. coli* K-12 (2×10^5 cfu/mL, 50 mL) with different scavengers (0.05 mmol/L Cr(VI): e^- scavenger, 0.5 mmol/L isopropanol: $\bullet OH_{bulk}$ scavenger, 0.5 mmol/L sodium oxalate: h^+ scavenger, 0.1 mmol/L Fe(II)-EDTA: H_2O_2 scavenger) in the presence of BV-NT (100 mg/L) under VL irradiation. No inactivation occurs in the dark and light controls.

dx.doi.org/10.1021/es2042977 | Environ. Sci. Technol. 2012, 46, 4599–4606

indicates that reactive species generated from the reduction site, such as e^- and $\bullet O_2^-$, are not the major reactive species. In the presence of Fe(II) to remove H_2O_2, the inactivation efficiency is moderately decreased, suggesting H_2O_2 is involved in the bacterial inactivation. Interestingly, with the addition of sodium oxalate to remove the h^+, the photocatalytic bacterial inactivation is almost completely inhibited, indicating the oxidation pathway is dominant in the VLD photocatalytic bacterial inactivation by BV-NT. Since h^+ will react with surface adsorbed hydroxyl groups (OH^-) or water to yield surface adsorbed hydroxyl radical ($\bullet OH_{ads}$), the major reactive species for the VLD photocatalytic inactivation by BV-NT could be h^+, $\bullet OH_{ads}$, or both.

To study the role of $\bullet OH_{ads}$ in the photocatalytic inactivation, an F^- surface modification was used to remove the $\bullet OH_{ads}$ because fluoride shows strong and stable adsorption on photocatalyst and the concentration of surface OH^- on the photocatalyst can be minimized by adopting fluoride-exchange.[22] With the substitution of surface OH^- for fluoride, the production of $\bullet OH_{ads}$ can be significantly reduced. The XPS spectrum of F^- surface modified BV-NT powder prepared by adding NaF (5 mmol/L) in the aqueous BV-NT suspension (100 mg/L), filtering, and drying confirms that F is successfully adsorbed on the BV-NT surface (Figure S3). No distinct difference in bacterial adsorption is found, indicating the affinity of bacterial cells to photocatalyst surface remains no change before and after F^- surface modification. With 5 mmol/L F^- modification, the inactivation efficiency is significantly decreased, indicating the $\bullet OH_{ads}$ is important for the VLD photocatalytic bacterial inactivation (Figure S4). It should be noted that, after F^- surface modification, the decrease of $\bullet OH_{ads}$ may promote the production of $\bullet OH_{bulk}$.[23,24] However, in the present study, no enhancement effect for the inactivation efficiency is observed, suggesting $\bullet OH_{bulk}$ does not involved in VLD photocatalytic bacterial inactivation by BV-NT.

To study the role of h^+, first, argon (Ar) was aerated in the system to remove O_2 and hence eliminated any influence of reactive oxidative species from the conduction band, leaving only the function of valence band. Then, with F^- surface modification, the production of $\bullet OH_{ads}$ was interrupted. In the valence band, absorbed water is initially oxidized by h^+, and the resulting $\bullet OH$ combines with a second $\bullet OH$ to form H_2O_2, giving the total reaction being expressed as h^+ oxidizes H_2O (or OH^-) to produce H_2O_2.[25−27] So the addition of F^- plus isopropanol can mostly disable the functions of both $\bullet OH_{ads/bulk}$ and H_2O_2, leaving the function of h^+ alone. As shown in Figure 3, to make the contribution more obvious, a sequential scavenger study is performed by adding sodium oxalate after 1 h of VL irradiation. It is found that with this h^+ scavenger (sodium oxalate) addition, the inactivation efficiency is gradually decreased. About 3.5 log of bacterial population still remains after 5 h of VL irradiation. There is a possibility that F^- plus isopropanol may not be sufficient to remove the continuously generating $\bullet OH_{ads}$ and $\bullet OH_{bulk}$. Thus, a new batch of F^- plus isopropanol is also added in both cases with and without sodium oxalate addition, and no difference inactivation efficiency is found except that with sodium oxalate is employed. No inactivation occurs in dark and light controls under Ar aeration with the addition of multiple scavengers (Figure S5). This result indicates that when removing the h^+ alone, the inactivation is inhibited, proving that the h^+ alone can directly inactivate the bacterial cells.

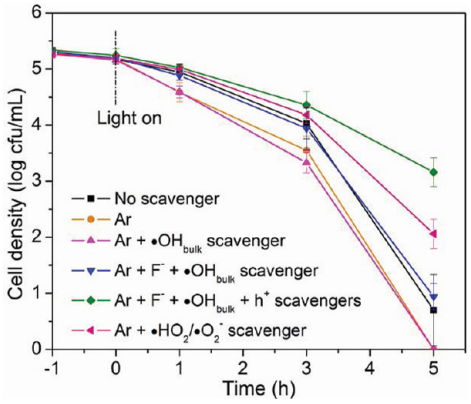

Figure 3. Photocatalytic inactivation efficiency of *E. coli* K-12 (2×10^5 cfu/mL, 50 mL) under different scavenger conditions (0.5 mmol/L isopropanol: $\bullet OH_{bulk}$ scavenger, 0.5 mmol/L sodium oxalate: h^+ scavenger, 2 mmol/L TEMPOL: $\bullet HO_2/\bullet O_2^-$ scavenger) with F^- surface modification (5 mmol/L NaF) and Ar aeration by BV-NT (100 mg/L) under VL irradiation. The oxalate is added after 1 h of VL irradiation.

The above results indicate that $\bullet OH_{ads}$ is more important than $\bullet OH_{bulk}$ in the photocatalytic process, probably due to the extremely short life-span of $\bullet OH_{bulk}$, which is supposed to be quickly quenched in the aqueous media before it can cause any damage to the bacterial cell. In the present system, the reduction pathway is not important, but moderate inhibition of inactivation is clearly observed by using H_2O_2 scavenger (Figure 2), suggesting a small amount of H_2O_2 may be produced from valence band. As discussed above, H_2O_2 in the valence band is believed to be mainly initiated by coupling of two $\bullet OH$.[25−27] It has been found that both $\bullet OH_{ads}$ and $\bullet OH_{bulk}$ can combine to produce H_2O_2,[8] which can subsequently react with $\bullet OH$ to form protonated superoxide radical ($\bullet HO_2$)[28,29] that function like $\bullet O_2^-$ to inactivate the bacterial cells. Thus, $\bullet OH_{ads}$ is suggested to play a crucial role in the production of H_2O_2 and $\bullet HO_2$ in the valence band, with initial resulting species in close contact with BV-NT interface (eqs 1−3)

$$h^+ + OH^-_{ads} \rightarrow \bullet OH_{ads} \quad (1)$$

$$\bullet OH_{ads} + \bullet OH_{ads} \rightarrow H_2O_2 \quad (2)$$

$$H_2O_2 + \bullet OH_{ads} \rightarrow \bullet HO_2 + H_2O \quad (3)$$

To confirm this process, 4-hydroxy-2,2,6,6-tetramethylpiperidinyloxy (TEMPOL) was used as the superoxide ($\bullet O_2^-$ and $\bullet HO_2$) scavenger.[30] Under Ar aeration, the addition of TEMPOL obviously reduces the photocatalytic inactivation efficiency, confirming that $\bullet HO_2$ can be produced from the valence band and act as inactivation reactive species (Figure 3). This result matches well with the observation of $\bullet O_2^-$ formation in the valence band by h^+ trapping reactions,[31] as $\bullet O_2^-$ can quickly transform to $\bullet HO_2$ in aqueous media.[32] Figure 3 also shows considerable enhancement in inactivation efficiency when adopting anaerobic condition in which no O_2 is to be used as e^- acceptor. Thus, in the bacterial inactivation system by BV-NT, the important e^- trapping to prevent the recombination of e^--h^+ pair is more likely to be achieved by the bacterial cell itself by directly injecting e_{cb}^- into the bacteria and leading to the damage of cell membrane,[20] because O_2 cannot be an effective e^- acceptor in the present system. The fact that

dx.doi.org/10.1021/es2042977 | Environ. Sci. Technol. 2012, 46, 4599−4606

no distinct inhibition effect is observed with F^- surface modification under anaerobic condition is another evidence that the bacterial inactivation effect of e^- compensates the role of $\bullet OH_{ads}$. To further confirm the direct function of e^-, in the presence of oxalate under anaerobic condition, Cr(VI) is added, and the decease of inactivation efficiency is clearly observed (Figure S6). However, the fact that removing e^- by Cr(VI) can increase the inactivation efficiency under aerobic condition suggests that the function of e^- as a disinfection agent is only a minor part under aerobic condition and is readily suppressed by the inactivation promotion effect of preventing the recombination of e^--h^+ pair in the presence of an effective e^- scavenger. Meanwhile, a more severe inhibition effect of inactivation is observed by removing $\bullet OH_{ads}$, compared with removing H_2O_2 or $\bullet HO_2$ alone, indicating that besides indirect involvement, the $\bullet OH_{ads}$ may also have a direct inactivation effect toward bacterial cells. Because the $\bullet OH_{ads}$ can readily abstract hydrogen atom from membrane lipids at a diffusion-controlled rate, leading to the formation of carbon-centered radicals which can penetrate the lipid bilayer down to the upper portion of the lipid slab and cause damage to the proteins and fatty acids.[33]

3.2.2. Role of Direct Contact Effect. To further investigate whether the direct contact between photocatalyst and bacterial cell was required for an effective inactivation, the inactivation experiment was conducted with the partition system. The *E. coli* K-12 suspension is added into the semipermeable membrane container, and the BV-NT is dispersed outside of the membrane container. The semipermeable membrane has a molecular weight cutoff (MWCO) of 12000−14000 Da, corresponding to a pore size less than 5 nm. The obtained nanotube has hexagonal cross sections with length of about 1.2 μm and width of 200 nm, and the rod-shaped *E. coli* K-12 cell is about 2.0 μm long and 0.5 μm in diameter. Therefore, both species cannot pass through the membrane pore, and the direct contact between bacterial cell and photocatalyst is prohibited. Only about 0.8 log-reduction of bacterial cells is achieved inside the partition system after 5 h of VL irradiation (Figure S7), suggesting the inactivation is mostly inhibited, which indicates the direct contact between photocatalyst and bacterial cell is very important in the BV-NT system. To further investigate the 0.8 log-reduction of bacterial population, the inactivation time is prolonged to 10 h (Figure S8). It was found that the addition of isopropanol also had no significant influence on the inactivation efficiency, indicating that the bacterial inactivation by BV-NT in the partition system is not caused by $\bullet OH_{bulk}$. The average lifetime for $\bullet OH$ is about 4×10^{-9} s, and the diffusion distance of $\bullet OH$ in water has been estimated to be only about 6 nm.[34] Thus it is virtually impossible for $\bullet OH$ to traverse the separating membrane with a thickness of 25−50 μm. The diffusion distance estimated seems even insufficient for directly attacking the bacterial cells, unless they are in very close contact onto the photocatalyst surface. The addition of Fe(II) significantly inhibits the photocatalytic inactivation process, indicating that the inactivation in partition system is actually caused by the diffusing H_2O_2. Moreover, Cr(VI) and sodium oxalate are added to quench the H_2O_2 production from reduction and oxidation sites, respectively. It is found that when interrupting the H_2O_2 generation pathway of reduction site by Cr(VI), the inactivation efficiency in the partition system remains unchanged as compared with no scavenger, while interrupting the H_2O_2 generation pathway of oxidation site by sodium oxalate, the photocatalytic inactivation is significantly inhibited and the efficiency is the same as with the Fe(II) scavenger. These results further confirm that the reduction pathway is not important, and H_2O_2 in the photocatalytic BV-NT system is mainly produced from the oxidation site.

3.3. Destruction Model of Bacterial Cells. To understand the destruction model of bacterial cells in the BV-NT photocatalytic system under VL irradiation, the structure and morphology of *E. coli* K-12 at the different stages of photocatalytic inactivation was examined by TEM studies (Figure 4). Before the photocatalytic inactivation, the cell of *E. coli* K-12 exhibits evenly rendered interior with a well-defined cell wall (Figure 4A). After 10 h irradiation (Figure 4B), the central portion (cytoplasm) of the cell is still intact but part of the cell wall structure appears obscure, indicating initial damage to the cell wall and cytoplasmic membrane. Potassium ion (K^+), a component virtually existing in bacterial cells and involving in the regulation of polysome content and protein synthesis, quickly leaks from the bacterial cells during the inactivation process (Figure S9), because of the permeability change of membrane, resulting in the loss of cell viability.[35] When further increasing the VL irradiation time to 20 h, part of the cell wall and cytoplasmic membrane is completely destroyed with an even more severe leakage of the intracellular components (Figure 4C). Finally, after 32 h of VL irradiation, the cell becomes almost translucent, leaving only a distortional shape of the cell wall with little cytoplasmic components inside the cell (Figure 4D). This observation indicates that the destruction process of the cell is to begin from the cell wall to other cellular components. Due to the crucial role of direct contact between bacterial cell and BV-NT, the first attack site of bacterial cell is expected to be the cell wall and cytoplasmic membrane. Before the cell wall is ruptured, the cytoplasmic components will remain intact inside the cell. Therefore, the inactivation efficiency is relatively low at the very beginning and followed by a dramatic increase when the cell wall is destroyed after 20 h irradiation (Figure S10).

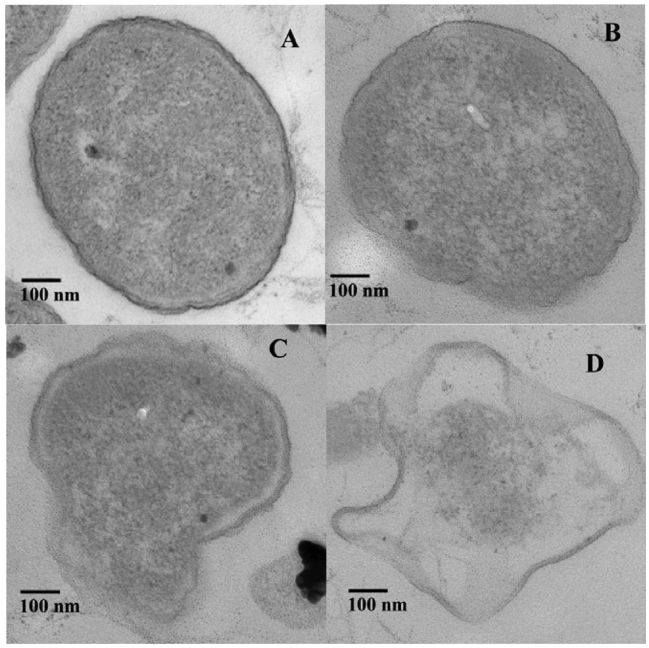

Figure 4. TEM images of *E. coli* K-12 (2×10^7 cfu/mL, 50 mL) photocatalytically treated with BV-NT (100 mg/L) under VL irradiation. (A) 0 h, (B) 10 h, (C) 20 h, and (D) 32 h.

Based on all the above results, the overall mechanism leading to the VLD photocatalytic inactivation of *E. coli* K-12 in the BV-NT system is proposed (Figure 5), which prevails especially

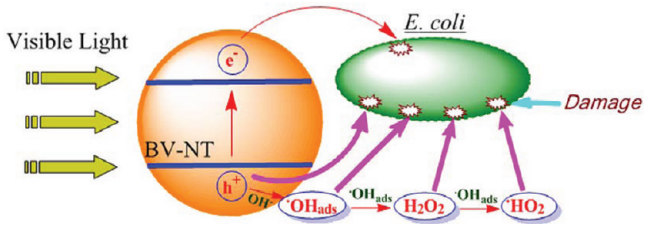

Figure 5. Schematic illustration of photocatalytic inactivation of *E. coli* K-12 process by BV-NT under VL irradiation.

in photocatalytic inactivation under anaerobic condition. The major reactive species is photogenerated h^+ and the reactive oxidative species (i.e., $\bullet OH_{ads}$, H_2O_2, and $\bullet HO_2/\bullet O_2^-$) derived from the h^+, which can contact and inactivate the bacterial cells in a nonpartition system, while only a limited amount of H_2O_2 can diffuse into the membrane chamber to act as a long-range disinfection agent in the partition system. The photocatalytic inactivation mechanism in the BV-NT system is quite different from those in our previous studies, in which the direct contact is not required for the inactivation, and $\bullet OH_{bulk}$ or H_2O_2 is the dominant active species.[8,17,21] It can be rationalized by considering the specific band structure of $BiVO_4$. The conduction band and valence band edges of $BiVO_4$ at the point of zero charge (pH_{zpc}) are estimated to be 0.31 and 2.76 eV, respectively.[36] Because of the low-lying conduction band position, it is difficult for $BiVO_4$ to reduce O_2 acting as the electron acceptor in other usual photocatalytic reactions.[37] Overall water splitting has not been observed, and high efficient photocatalytic oxygen evolution and degradation of alkylphenols are only occurring in the modified systems containing additional electron acceptor, such as Ag^+.[4,38,39] Therefore, the reduction site is less important and the oxidation site controls the photocatalytic inactivation activity of BV-NT by generating diffusing H_2O_2, which is highly responsible for an effective inactivation without direct contact with photocatalyst, only to be produced from valence band. After possible quenching by $\bullet OH_{ads}$ and e^-, the remaining H_2O_2 for bacterial inactivation will be further reduced. The POD/DPD method has been used to detect the concentration of formed H_2O_2 in this photocatalytic system.[12,20] However, the detected H_2O_2 concentration is so small that beyond the detection limit. To further confirm the existence of H_2O_2 attacking, the activity change of bacterial catalase (CAT), a well-known antioxidant enzyme that defends against oxidative stress from the environment, is investigated in the partition system during VLD photocatalytic inactivation. CAT catalyzes the decomposition of H_2O_2 to water and oxygen. As CAT is an enzyme to protect bacterial cells from H_2O_2 damage, a higher CAT activity implies that bacterial cells are encountering a more significant H_2O_2 attack from photocatalytic treatment. In the initial 2 h, CAT activity is found to increase rapidly with time (Figure S11), indicating a considerable amount of H_2O_2 is attacking the bacterial cells at the very beginning and the bacterial defense system induces a higher level of CAT in order to against the oxidative stress of H_2O_2. This observation matches well with the low inactivation efficiency in the first 3 h because antioxidative enzyme such as CAT is protecting the bacterial cells (Figure S7). After 3 h of VL irradiation, the CAT activity begins to drop and the inactivation efficiency is increasing, indicating the oxidative stress from H_2O_2 evolved by BV-NT exceeds the protection ability of the bacterial defense system, leading to the loss of viability of the bacterial cells.

3.4. Analysis of Radical Production. The generation of $\bullet OH_{bulk}$ was investigated through the method of photoluminescence with terephthalic acid. It was found that no $\bullet OH_{bulk}$ was detected, further confirming the absence of $\bullet OH_{bulk}$ in the BV-NT-VL system, although the $\bullet OH_{bulk}$ was detected in the UV-irradiated TiO_2 system (Figure 6). In the usual photocatalytic system, such as UV-irradiated TiO_2, large amounts of $\bullet OH_{bulk}$ can be produced by any secondary events,[40] such as the decomposition of H_2O_2 and the well-known Harber-Weiss reaction,[27,41] in which H_2O_2 reacts with $\bullet O_2^-$ to give $\bullet OH_{bulk}$ directly in bulk solution, without a radical releasing process from photocatalyst surface. However, in the present system, the reduction site is less important, and the oxidation site controls the photocatalytic disinfection activity, resulting in very limited role of H_2O_2 and $\bullet O_2^-$. Therefore, the production of $\bullet OH_{bulk}$ is significantly interrupted; however, exactly indicating the fact that $\bullet OH_{ads}$ cannot be freed in the bulk solution very easily. Several previous studies have focused on the bactericidal effects of $\bullet OH$, but few of them have distinguished the exact role of $\bullet OH_{ads}$ and $\bullet OH_{bulk}$. In the BV-NT-VL system, it is found that $\bullet OH_{bulk}$ may not be the bactericidal agent and $\bullet OH_{ads}$ instead is the major reactive species both directly and indirectly involved in inactivation

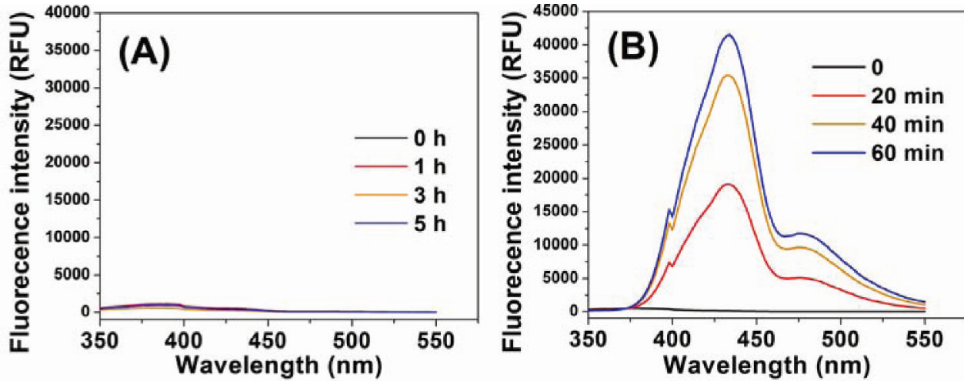

Figure 6. Fluorescence emission spectral changes observed during the irradiation of (A) the BV-NT with VL irradiation and (B) P25-TiO_2 with UV irradiation in a 4×10^{-4} mol/L terephthalic acid and 2×10^{-3} mol/L NaOH (excitation at 315 nm).

dx.doi.org/10.1021/es2042977 | Environ. Sci. Technol. 2012, 46, 4599–4606

process at close contact with the photocatalyst (within the diffuse Gouy−Chapman layer). While our findings will not preclude the possibility that some of these initially adsorbed $\bullet OH_{ads}$ are subsequently released into the bulk solution and become free radicals as suggested in some early publications,[42] we consider this possible releasing is very unlikely.

In summary, BV-NT was found to be highly photoactive under VL irradiation for bacterial inactivation in water without any bacterial regrowth, indicating its great potential to be applied in high-efficient environmental water disinfection. The photogenerated h^+ and its secondary resulting species, such as $\bullet OH_{ads}$, H_2O_2, and $\bullet HO_2/\bullet O_2^-$, were the major reactive species, guaranteeing the strong oxidation activity toward the bacterial cells. These species were supposed to be confined in close contact with the photocatalyst surface. In particular, the bacterial cell is found to act as an e^- acceptor to prevent e^--h^+ recombination, especially for disinfection under anaerobic condition. Further research will focus on elucidating the fundamental role of photogenerated e^- acting as bacterial inactivation agent. These findings are encouraging and will lead to the development of new insights into understanding the mechanisms of bacterial inactivation by VLD photocatalysis. The research methodology of various scavenging effects combined with partition system in this study will be established as a useful and versatile methodology for mechanism investigation, thus developing suitable protocol for environmental disinfection based on different mechanisms.

■ ASSOCIATED CONTENT

Supporting Information

Setup of partition system, XPS spectrum, K^+ leakage, CAT activity, photocatalytic disinfection with cell concentration of 2×10^7 cfu/mL, with F^- modification, with oxalate and Cr(VI) under anaerobic condition, in partition system with and without scavengers, and dark and light control experiments. This material is available free of charge via the Internet at http://pubs.acs.org.

■ AUTHOR INFORMATION

Corresponding Author

*Phone: +86 27 6786 7037. Fax: +86 27 6786 1185. E-mail: yuying@phy.ccnu.edu.cn (Y.Y.). Phone: +852 3943 6383. Fax: +852 2603 5767. E-mail: pkwong@cuhk.edu.hk (P.K.W.).

Notes

The authors declare no competing financial interest.

■ ACKNOWLEDGMENTS

The project was supported by a research grant (GRF 476811) from the Research Grant Council, Hong Kong SAR Government to P. K. Wong, NSFC (20973070) to Y. Yu, and NSFC (21077104) to G. Y. Li and T. C. An.

■ REFERENCES

(1) Matsunaga, T.; Tomoda, R.; Nakajima, T.; Wake, H. Photoelectrochemical sterilization of microbial cells by semiconductor powders. *FEMS Microbiol. Lett.* **1985**, *29*, 211−214.

(2) Christensena, P. A.; Curtisb, T. P.; Egertona, T. A.; Kosaa, S. A. M.; Tinlina, J. R. Photoelectrocatalytic and photocatalytic disinfection of *E. coli* suspensions by titanium dioxide. *Appl. Catal., B* **2003**, *41*, 371−386.

(3) Kim, D. S.; Kwak, S. Y. Photocatalytic inactivation of *E. coli* with a mesoporous TiO_2 coated film using the film adhesion method. *Environ. Sci. Technol.* **2009**, *43*, 148−151.

(4) Kudo, A.; Omori, K.; Kato, H. A novel aqueous process for preparation of crystal form-controlled and highly crystalline $BiVO_4$ powder from layered vanadates at room temperature and its photocatalytic and photophysical properties. *J. Am. Chem. Soc.* **1999**, *121*, 11459−11467.

(5) Kohtani, S.; Koshiko, M.; Kudo, A.; Tokumura, K.; Ishigaki, Y.; Toriba, A.; Hayakawa, K.; Nakagaki, R. Photodegradation of 4-alkylphenols using $BiVO_4$ photocatalyst under irradiation with visible light from a solar simulator. *Appl. Catal., B* **2003**, *46*, 573−586.

(6) Zhang, L. S.; Wong, K. H.; Zhang, D. Q.; Hu, C.; Yu, J. C.; Chan, C. Y.; Wong, P. K. Zn:In$(OH)_yS_z$ solid solution nanoplates: synthesis, characterization, and photocatalytic mechanism. *Environ. Sci. Technol.* **2009**, *43*, 7883−7888.

(7) Cho, M.; Chung, H.; Choi, W.; Yoon, J. Different inactivation behaviors of MS-2 phage and *Escherichia coli* in TiO_2 photocatalytic disinfection. *Appl. Environ. Microbiol.* **2005**, *71*, 270−275.

(8) Wang, W. J; Zhang, L. S; An, T. C; Li, G. Y.; Yip, H. Y.; Wong, P. K. Comparative study of visible-light-driven photocatalytic mechanisms of dye decolorization and bacterial disinfection by B−Ni-codoped TiO_2 microspheres: The role of different reactive species. *Appl. Catal., B* **2011**, *108−109*, 108−116.

(9) Ren, L.; Jin, L.; Wang, J. B.; Yang, F.; Qiu, M.; Yu, Y. Template-free synthesis of $BiVO_4$ nanostructures: I. Nanotubes with hexagonal crosssections by oriented attachment and their photocatalytic property for water splitting under visible light. *Nanotechnology* **2009**, *20*, 115603.

(10) Ren, L.; Ma, L.; Jin, L.; Wang, J. B.; Qiu, M.; Yu, Y. Template-free synthesis of $BiVO_4$ nanostructures: II. Relationship between various microstructures for monoclinic $BiVO_4$ and their photocatalytic activity for the degradation of rhodamine B under visible light. *Nanotechnology* **2009**, *20*, 405602.

(11) Li, C.; Wang, F.; Zhu, J.; Yu, J. C. $NaYF_4$:Yb,Tm/CdS composite as a novel near-infrared-driven photocatalyst. *Appl. Catal., B* **2010**, *100*, 433−439.

(12) Bader, H.; Sturzenegger, V.; Hoigné, J. Photometric method for the determination of low concentrations of hydrogen peroxide by the peroxidase catalyzed oxidation of N,N-diethyl-p-phenylenediamine (DPD). *Water Res.* **1988**, *22*, 1109−1115.

(13) Cayman Chemical Company, Protocol for Catalase Assay; Ann Arbor: MI, USA, 2009.

(14) Rincón, A. G.; Pulgarin, C. Bactericidal action of illuminated TiO_2 on pure *Escherichia coli* and natural bacterial consortia: post-irradiation events in the dark and assessment of the effective disinfection time. *Appl. Catal., B* **2004**, *49*, 99−112.

(15) Jin, R.; Gao, W; Chen, J.; Zeng, H.; Zhang, F.; Liu, Z.; Guan, N. Photocatalytic reduction of nitrate ion in drinking water by using metal-loaded $MgTiO_3$-TiO_2 composite semiconductor catalyst. *J. Photochem. Photobiol., A* **2004**, *162*, 585−590.

(16) Zhang, L. S.; Wong, K. H.; Yip, H. Y.; Hu, C.; Yu, J. C.; Chan, C. Y.; Wong, P. K. Effective photocatalytic disinfection of *E. coli* K-12 using AgBr-Ag-Bi_2WO_6 nanojunction system irradiated by visible light: the role of diffusing hydroxyl radicals. *Environ. Sci. Technol.* **2010**, *44*, 1392−1398.

(17) Chen, Y. X.; Yang, S. Y.; Wang, K.; Lou, L. P. Role of primary active species and TiO_2 surface characteristic in UV-illuminated photodegradation of Acid Orange 7. *J. Photochem. Photobiol., A* **2005**, *172*, 47−54.

(18) Khodja, A. A.; Boulkamh, A.; Richard, C. Phototransformation of metobromuron in the presence of TiO_2. *Appl. Catal., B* **2005**, *59*, 147−154.

(19) Schrank, S. G.; José, H. J.; Moreira, R. F. P. M. Simultaneous photocatalytic Cr(VI) reduction and dye oxidation in a TiO_2 slurry reactor. *J. Photochem. Photobiol., A* **2002**, *147*, 71−76.

(20) Chen, Y. M.; Lu, A. H.; Li, Y.; Zhang, L. S.; Yip, H. Y.; Zhao, H. J.; An, T. C.; Wong, P. K. Naturally occurring sphalerite as a novel cost-effective photocatalyst for bacterial disinfection under visible light. *Environ. Sci. Technol.* **2011**, *45*, 5689−5695.

(21) Buxton, G. V.; Greenstock, C. L.; Helman, W. P.; Ross, A. B.; Tsang, W. Critical review of rate constants for reactions of hydrated

electrons, hydrogen atoms and hydroxyl radicals in aqueous Solution. *J. Phys. Chem. Ref. Data* **1988**, *17*, 513−886.
(22) Calza, P.; Pelizzetti, E. Photocatalytic transformation of organic compounds in the presence of inorganic ions. *Pure Appl. Chem.* **2001**, *73*, 1839−1848.
(23) Park, H.; Choi, W. Effects of TiO_2 Surface fluorination on photocatalytic reactions and photoelectrochemical behaviors. *J. Phys. Chem. B* **2004**, *108*, 4086−4093.
(24) Minero, C.; Mariella, G.; Maurino, D.; Vione, V.; Pelizzetti, E. Photocatalytic transformation of organic compounds in the presence of inorganic ions. 2. competitive reactions of phenol and alcohols on a titanium dioxide−fluoride system. *Langmuir* **2000**, *16*, 8964−8972.
(25) Sakai, H.; Baba, R.; Hashimoto, K.; Fujishima, A. Local detection of photoelectrochemically produced H_2O_2 with a "wired" horseradish peroxidase microsensor. *J. Phys. Chem.* **1995**, *99*, 11896−11900.
(26) Ranjit, K. T.; Willner, I.; Bossmann, S. H.; Braun, A. M. Lanthanide oxide-doped titanium dioxide photocatalysts: novel photocatalysts for the enhanced degradation of p-chlorophenoxyacetic acid. *Environ. Sci. Technol.* **2001**, *35*, 1544−1549.
(27) Kikuchi, Y; Sunada, K; Iyoda, T.; Hashimoto, K.; Fujishima, A. Photocatalytic bactericidal effect of TiO_2 thin films: dynamic view of the active oxygen species responsible for the effect. *J. Photochem. Photobiol., A* **1997**, *106*, 51−56.
(28) Harbour, J. R.; Hair, M. L. Radical intermediates in the photosynthetic generation of hydrogen peroxide with aqueous zinc oxide dispersions. *J. Phys. Chem.* **1979**, *83*, 652−656.
(29) Dodd, N. J. F.; Jha, A. N. photoexcitation of aqueous suspensions of titanium dioxide nanoparticles: an electron spin resonance spin trapping study of potentially oxidative reactions. *Photochem. Photobiol.* **2011**, *87*, 632−640.
(30) Lejeune, D.; Hasanuzzaman, M.; Pitcock, A.; Francis, J.; Sehgal, I. The superoxide scavenger TEMPOL induces urokinase receptor (uPAR) expression in human prostate cancer cells. *Mol. Cancer* **2006**, *5*, 21.
(31) Howe, R. F.; Gratzel, M. EPR observation of trapped electrons in colloidal titanium dioxide. *J. Phys. Chem.* **1985**, *89*, 4495−4499.
(32) Rincón, A. G.; Pulgarin, C. Effect of pH, inorganic ions, organic matter and H_2O_2 on *E. coli* K12 photocatalytic inactivation by TiO_2: Implications in solar water disinfection. *Appl. Catal., B* **2004**, *51*, 283−302.
(33) Gamliel, A.; Afri, M.; Frimer, A. A. Determining radical penetration of lipid bilayers with new lipophilic spin traps. *Free Radical Biol. Med.* **2008**, *44*, 1394−1405.
(34) Roots, R.; Okada, S. Estimation of life times and diffusion distances of radicals involved in X-ray-induced DNA strand scissions or killing of mammalian cells. *Radiat. Res.* **1975**, *64*, 306−320.
(35) Ren, J.; Wang, W. Z.; Zhang, L.; Chang, J.; Hu, S. Photocatalytic inactivation of bacteria by photocatalyst Bi_2WO_6 under visible light. *Catal. Commun.* **2009**, *10*, 1940−1943.
(36) Jiang, H. Q.; Endo, H.; Natori, H.; Nagai, M.; Kobayashi, K. Fabrication and photoactivities of spherical-shaped $BiVO_4$ photocatalysts through solution combustion synthesis method. *J. Eur. Ceram. Soc.* **2008**, *28*, 2955−2962.
(37) Naya, S.-i.; Tanaka, M.; Kimura, K.; Tada, H. Visible-light-driven copper acetylacetonate decomposition by $BiVO_4$. *Langmuir* **2011**, *27*, 10334−10339.
(38) Xi, G.; Ye, J. Synthesis of bismuth vanadate nanoplates with exposed {001} facets and enhanced visible-light photocatalytic properties. *Chem. Commun.* **2010**, *46*, 1893−1895.
(39) Kim, H. G.; Hwang, D. W.; Lee, J. S. An undoped, single-phase oxide photocatalyst working under visible light. *J. Am. Chem. Soc.* **2004**, *126*, 8912−8913.
(40) Mao, Y.; Schöneich, C.; Asmus, K. D. Identification of organic acids and other intermediates in oxidative degradation of chlorinated ethanes on TiO_2 surfaces en route to mineralization: a combined photocatalytic and radiation chemical study. *J. Phys. Chem.* **1991**, *95*, 10080−10089.
(41) Hirakawa, T.; Nosaka, Y. Properties of $\bullet O_2^-$ and $\bullet$OH formed in TiO_2 aqueous suspensions by photocatalytic reaction and the influence of H_2O_2 and some ions. *Langmuir* **2002**, *18*, 3247−3254.
(42) Peterson, M. W.; Turner, J. A.; Nozik, A. J. Mechanistic studies of the photocatalytic behavior of titania: particles in a photoelectrochemical slurry cell and the relevance to photodetoxification reactions. *J. Phys. Chem.* **1991**, *95*, 221−225.

Supporting information

Visible-light-driven Photocatalytic Inactivation of *E. coli* K-12 by Bismuth Vanadate Nanotubes: Bactericidal Performance and Mechanism

Wanjun Wang[1], Ying Yu[2,*], Taicheng An[3], Guiying Li[3], Ho Yin Yip[1], Jimmy C. Yu[4], and Po Keung Wong[1,*]

[1]*School of Life Sciences and* [4]*Department of Chemistry, The Chinese University of Hong Kong, Shatin, N.T., Hong Kong SAR, CHINA*

[2]*Institute of Nanoscience and Nanotechnology, Central China Normal University, Wuhan 430079, CHINA*

[3]*State Key Laboratory of Organic Geochemistry, Guangzhou Institute of Geochemistry, Chinese Academy of Sciences, Guangzhou 510640, CHINA*

---

[*]Corresponding authors: Tel: +86 27 6786 7037, Fax: +86- 27 6786 1185; E-mail: yuying@phy.ccnu.edu.cn (Y. Yu); and Tel: +852 3943 6383, Fax: +852 2603 5767, E-mail: pkwong@cuhk.edu.hk (P.K. Wong)

Contents:

Figures (11 figures)

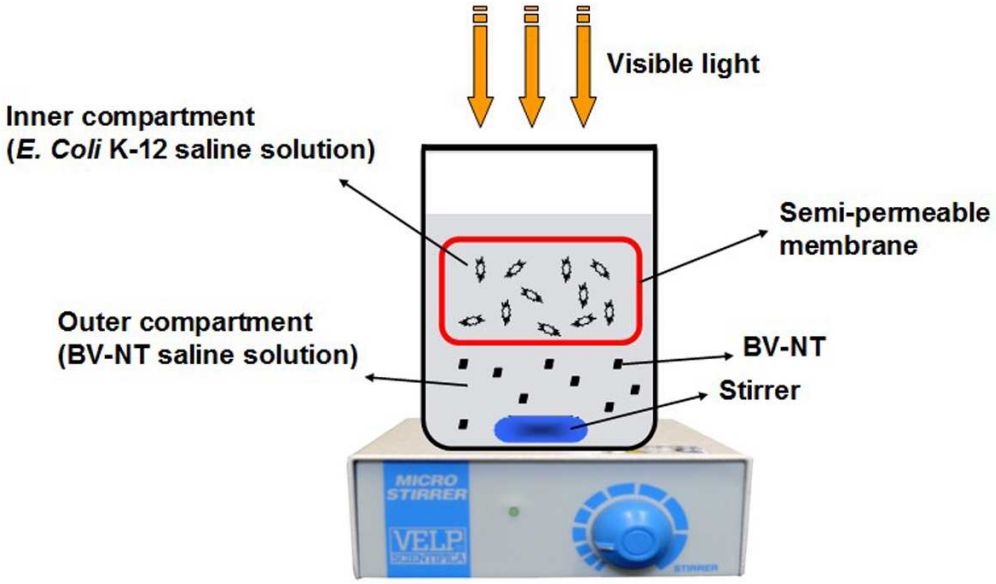

Figure S1. Schematic illustration of the partition system used in the photocatalytic inactivation with the BV-NT as photocatalyst under VL irradiation. Modified from that of Zhang et al. (2010)

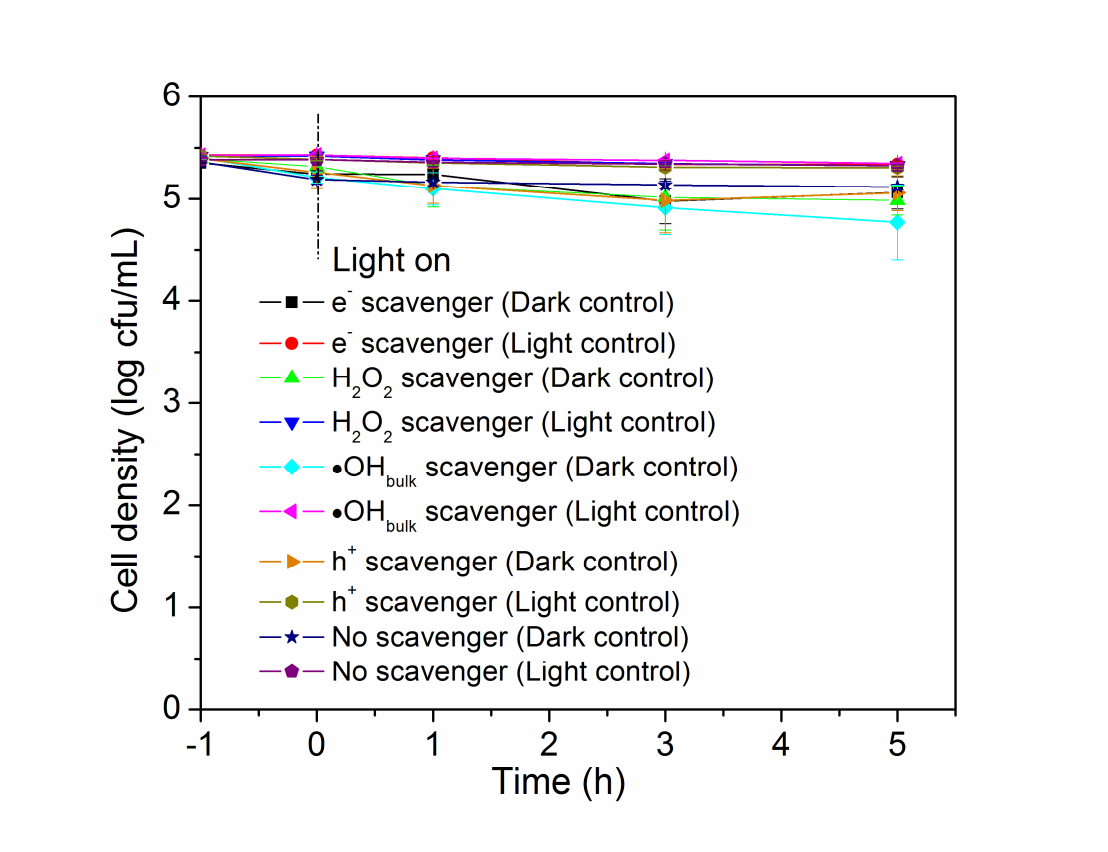

Figure S2. Photocatalytic inactivation efficiency of *E. coli* K-12 (2×10^5 cfu/mL, 50 mL) with different scavengers (0.05 mmol/L Cr(VI): e^- scavenger, 0.5 mmol/L isopropanol: $\bullet OH_{bulk}$ scavenger, 0.5 mmol/L sodium oxalate: h^+ scavenger, 0.1 mmol/L Fe(II)-EDTA: H_2O_2 scavenger) in the presence of BV-NT (100 mg/L) under VL irradiation in dark and light controls.

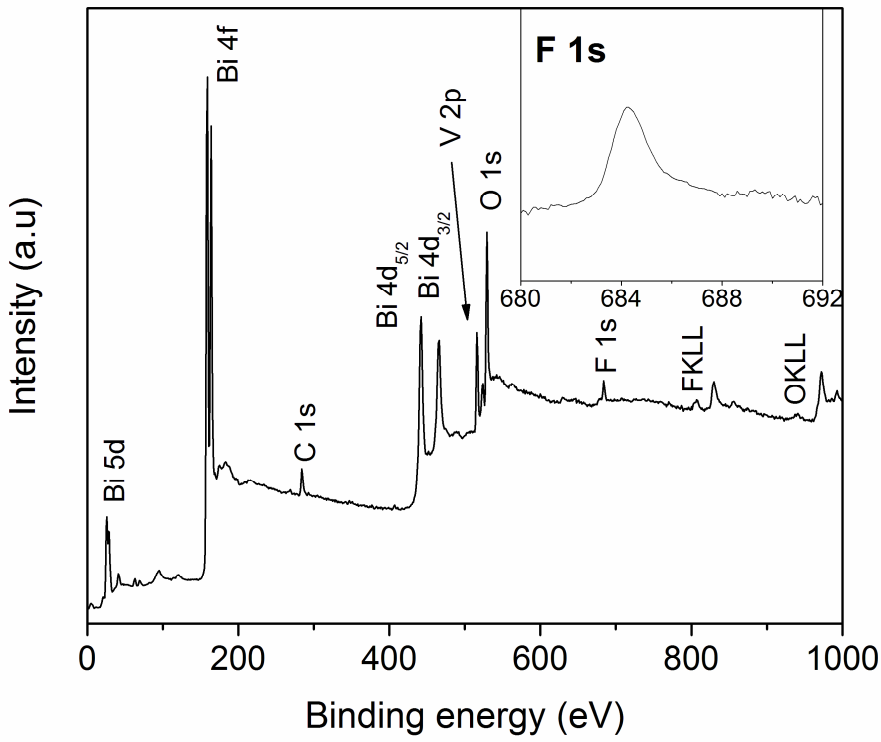

Figure S3. XPS spectrum of F^- surface modified BV-NT powder. The inset is high resolution spectra of F 1s for the fluorinated BV-NT.

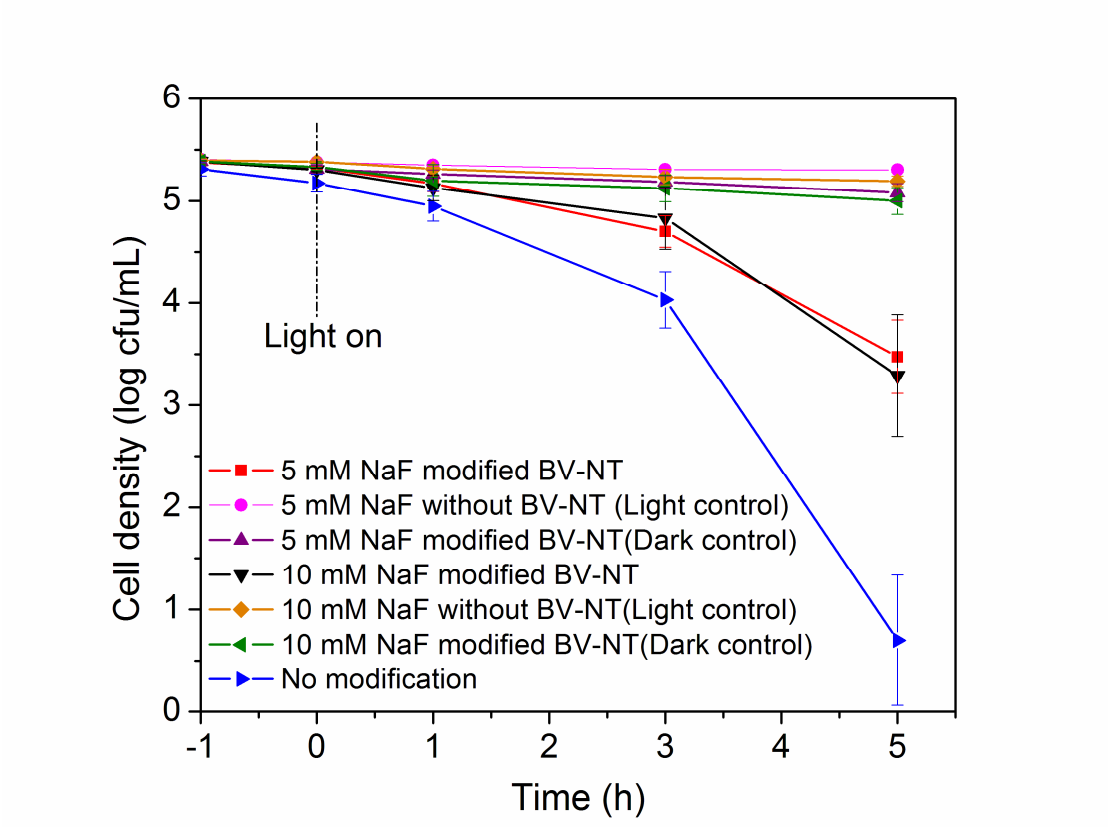

Figure S4. Photocatalytic inactivation efficiency of *E. coli* K-12 (2×10^5 cfu/mL, 50 mL) with different concentration of F^- surface modification by BV-NT (100 mg/L) under VL irradiation.

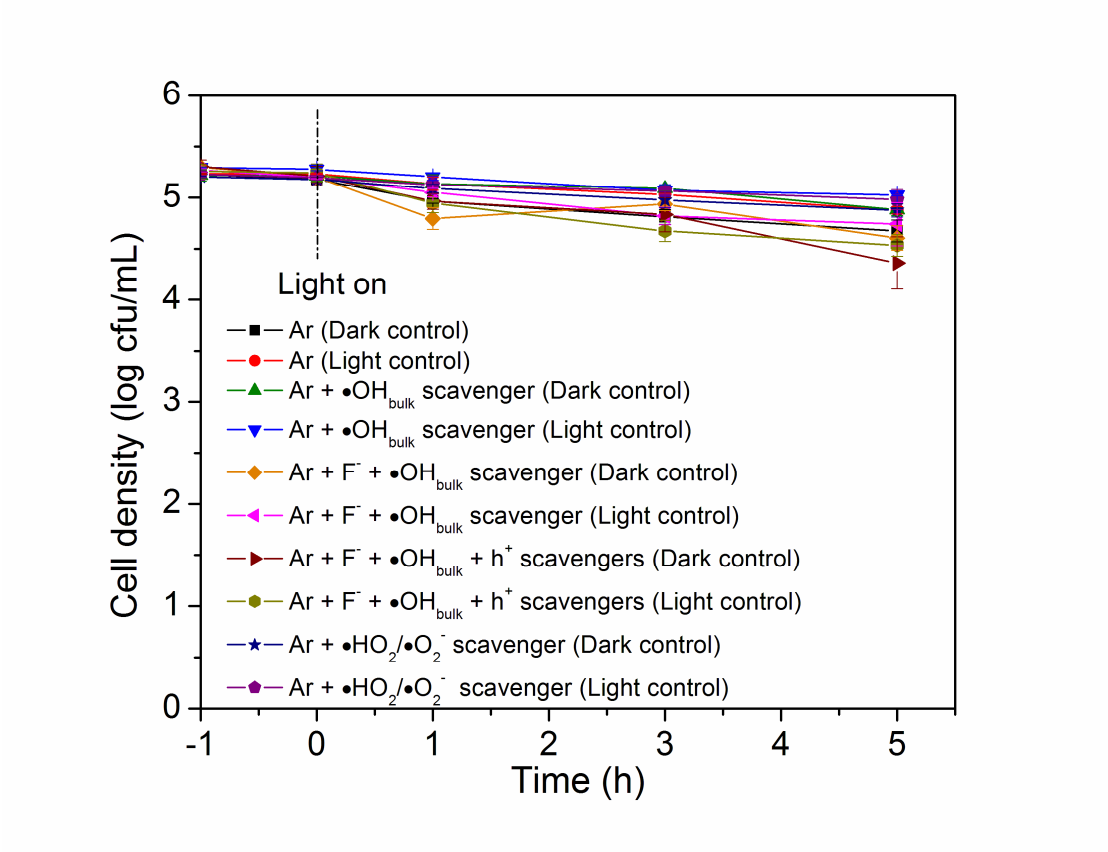

Figure S5. Photocatalytic inactivation efficiency of *E. coli* K-12 (2×10^5 cfu/mL, 50 mL) under different scavenger conditions (0.5 mmol/L isopropanol: •OH_{bulk} scavenger, 0.5 mmol/L sodium oxalate: h^+ scavenger, 2 mmol/L TEMPOL: •HO_2/•O_2^- scavenger) with F^- surface modification (5 mmol/L NaF) and Ar aeration by BV-NT (100 mg/L) under VL irradiation in dark and light controls. The oxalate is added after 1 h of VL irradiation.

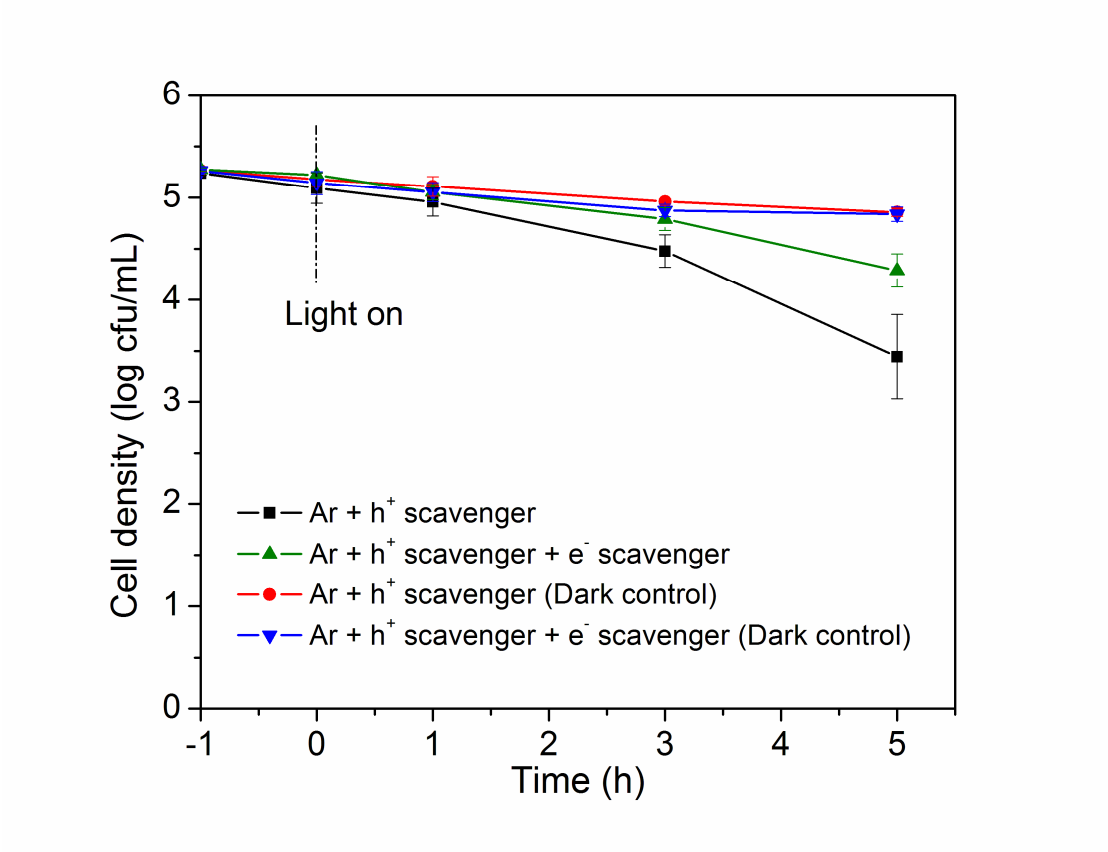

Figure S6. Photocatalytic inactivation efficiency of *E. coli* K-12 (2×10^5 cfu/mL, 50 mL) by BV-NT (100 mg/L) in the presence of 0.5 mmol/L sodium oxalate (h^+ scavenger) and 0.05 mmol/L Cr(VI) (e^- scavenger) under anaerobic condition. The Cr (VI) is added after 1 h of VL irradiation.

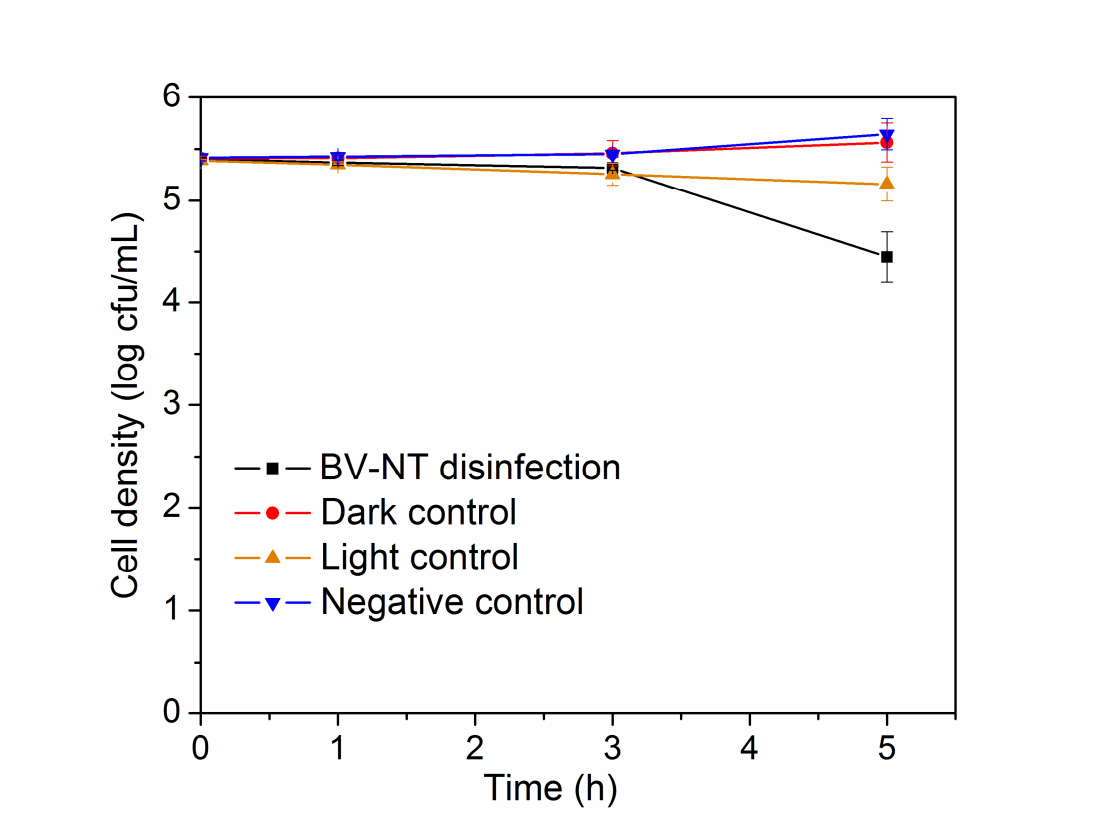

Figure S7. Photocatalytic inactivation efficiency of E. coli K-12 (2×10^5 cfu/mL, 20 mL) in the inner compartment of the partition system. The outer compartment is the BV-NT suspension (100 mg/L) under VL irradiation.

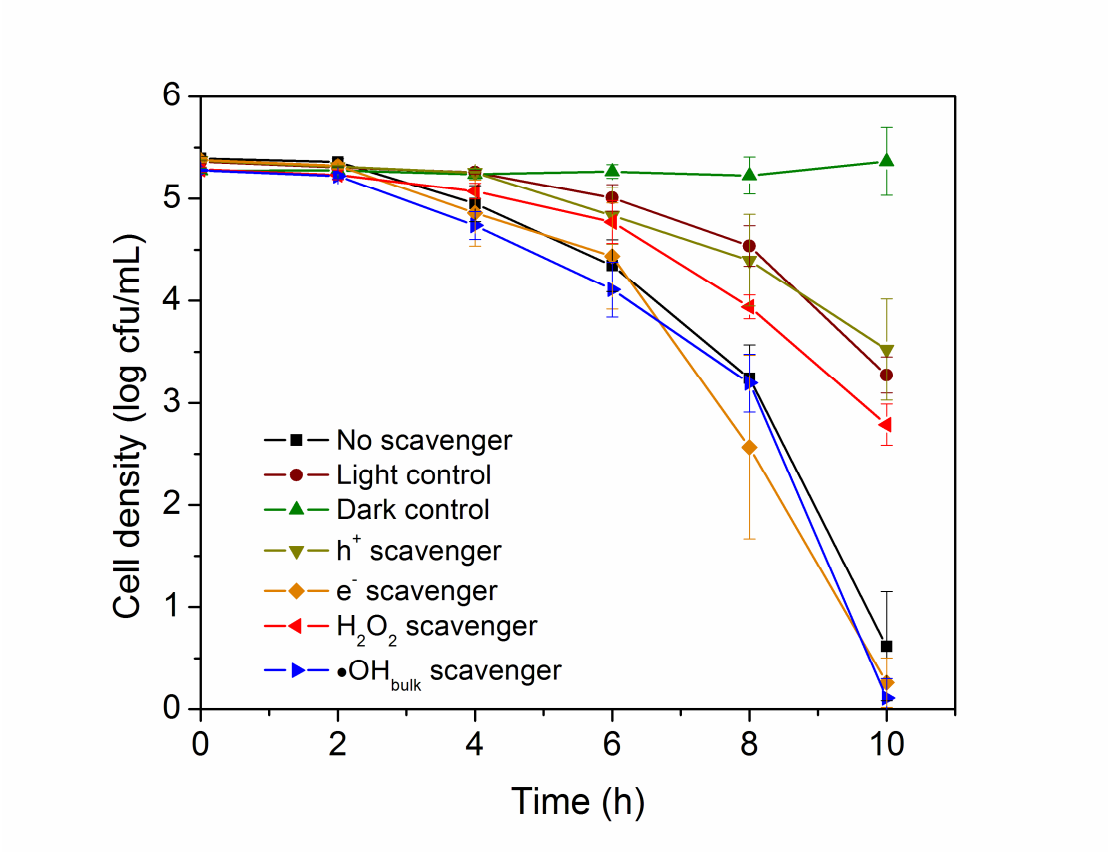

Figure S8. Photocatalytic inactivation efficiency of *E. coli* K-12 (2×10^5 cfu/mL, 20 mL) in the inner compartment of the partition system. The outer compartment is the BV-NT suspension (100 mg/L) with the addition of different scavengers (0.05 mmol/L Cr(VI): e^- scavenger, 0.5 mmol/L sodium oxalate: h^+ scavenger, 0.1 mmol/L Fe(II)-EDTA: H_2O_2 scavenger) under VL irradiation.

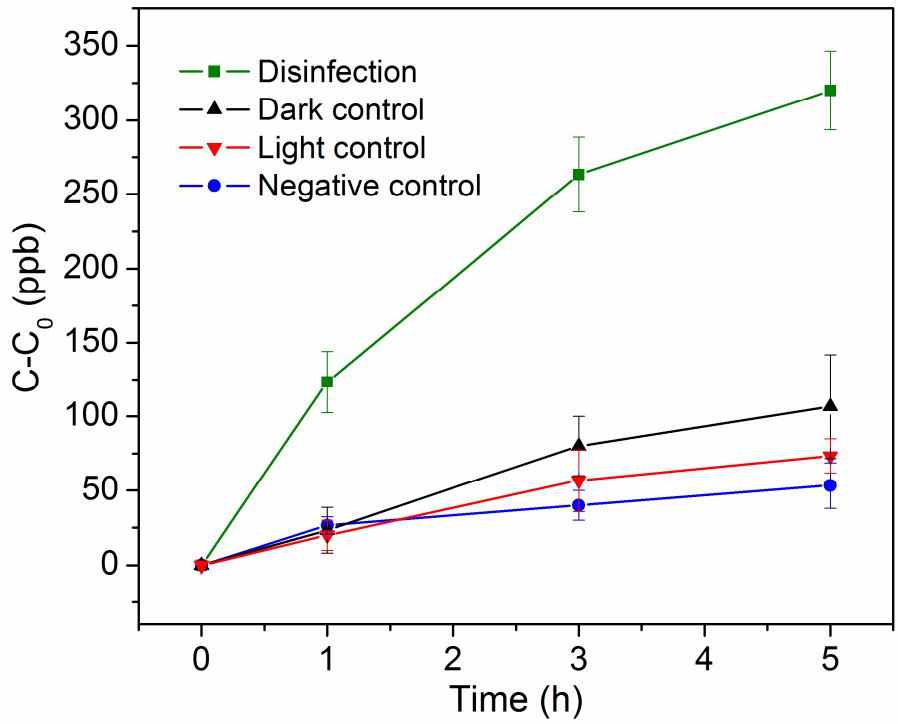

Figure S9. Potassiumion (K^+) leakage from *E. coli* K-12 (2×10^5 cfu/mL, 50 mL) during VLD photocatalytic inactivation by BV-NT (100 mg/L).

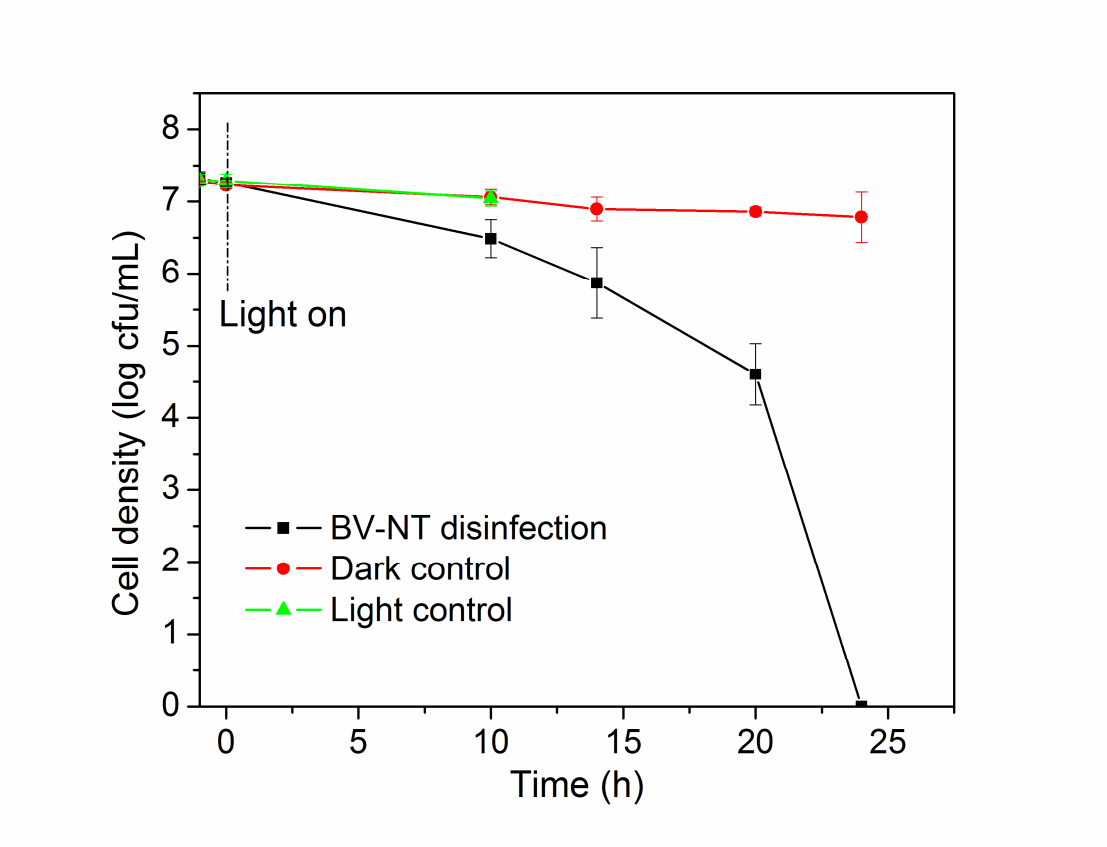

Figure S10. Photocatalytic inactivation efficiency of *E. coli* K-12 (2×10^7 cfu/mL, 50 mL) in the presence of BV-NT (100 mg/L) under visible light irradiation.

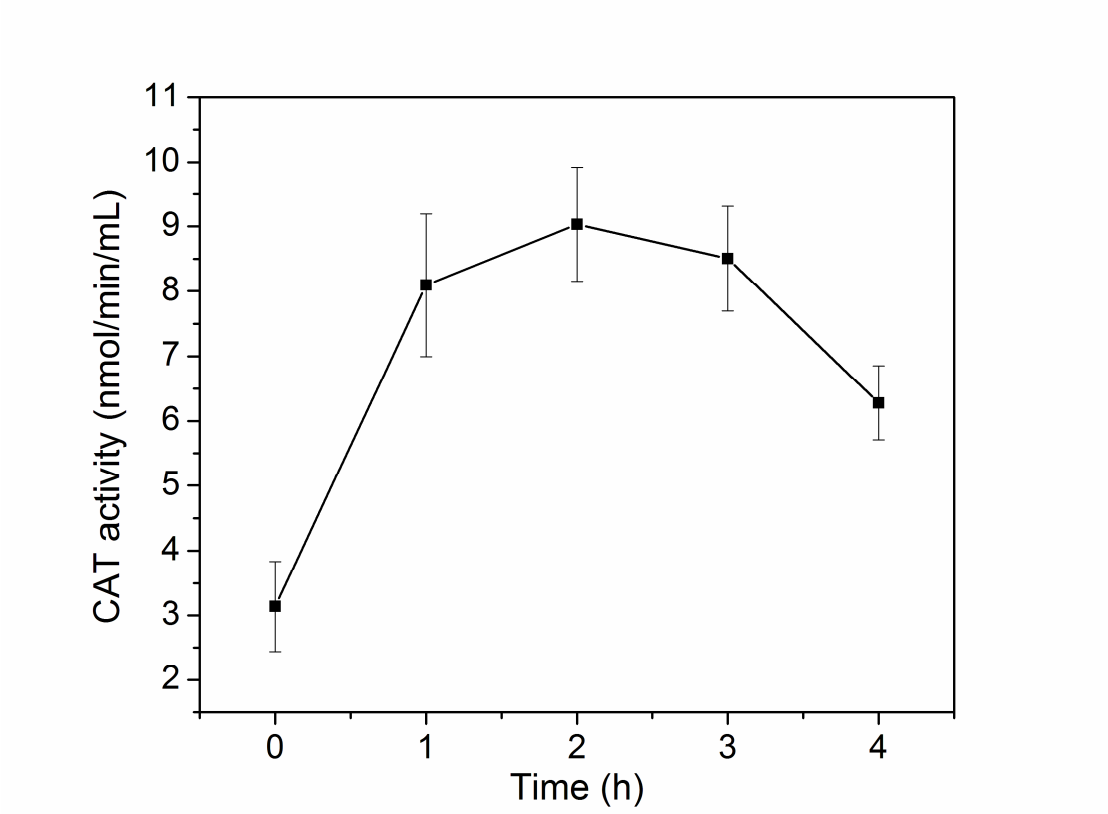

Figure S11. Induction of CAT activity under photocatalytic inactivation of *E. coli* K-12 by BV-NT under VL irradiation.